ELECTRONICS

Bend, stretch, and touch: Locating a finger on an actively deformed transparent sensor array

Mirza Saquib Sarwar, Yuta Dobashi, Claire Preston, Justin K. M. Wyss, Shahriar Mirabbasi, John David Wyndham Madden*

The development of bendable, stretchable, and transparent touch sensors is an emerging technological goal in a variety of fields, including electronic skin, wearables, and flexible handheld devices. Although transparent tactile sensors based on metal mesh, carbon nanotubes, and silver nanowires demonstrate operation in bent configurations, we present a technology that extends the operation modes to the sensing of finger proximity including light touch during active bending and even stretching. This is accomplished using stretchable and ionically conductive hydrogel electrodes, which project electric field above the sensor to couple with and sense a finger. The polyacrylamide electrodes are embedded in silicone. These two widely available, low-cost, transparent materials are combined in a three-step manufacturing technique that is amenable to large-area fabrication. The approach is demonstrated using a proof-of-concept 4 × 4 cross-grid sensor array with a 5-mm pitch. The approach of a finger hovering a few centimeters above the array is readily detectable. Light touch produces a localized decrease in capacitance of 15%. The movement of a finger can be followed across the array, and the location of multiple fingers can be detected. Touch is detectable during bending and stretch, an important feature of any wearable device. The capacitive sensor design can be made more or less sensitive to bending by shifting it relative to the neutral axis. Ultimately, the approach is adaptable to the detection of proximity, touch, pressure, and even the conformation of the sensor surface.

INTRODUCTION

As electronic devices become smaller, lighter, and multifunctional, there is a drive to integrate them into our clothes (*1*) or apply them on our skin (*2*) to unobtrusively monitor our health (*3*) and track our motions (*4*). These applications demand high conformability, motivating interest in so-called electronic skin (*5*) and, more recently, "ionic skin" (*6*). On the sensing side, devices have shown the ability to either detect touch (*7*–*10*), stretch (*11*–*14*), bend (*15*), or touch and stretch, without the ability to distinguish between the two (*6*, *15*). Several approaches have been taken to show stretchable devices, which often involve elastomer substrates combined with deformable electrodes consisting of carbon nanotubes (CNTs) (*14*–*17*), thin deformable single-crystal silicon structures (*18*), liquid metal (*19*), nanowires (*8*), and ionically conductive hydrogels (*6*). Changes in device geometry induced by mechanical deformation (for example, a touch) are typically detected as variations in an electrical property of the device such as capacitance or resistance. Ideally, a wearable device can operate while being simultaneously deformed.

In our case, we aim to detect the presence of a finger, as is done in a touch pad or touch screen. A challenge is that capacitance and resistance are affected by stretch, bend, and the pressure of touch. Here, we achieve some immunity to mechanical deformation in a touch sensor by making use of so-called projected electric fields that extend beyond the device to couple with and enable detection of a nearby finger (Fig. 1A). The approach of the finger leads to a drop in capacitance between the electrodes. The drop occurs because the electric field, whose strength is indicated by color, is increasingly directed toward the finger, reducing the charge shared between the two electrodes. This type of proximity sensing is well established in rigid indium tin oxide–based sensor devices and is known as mutual capacitive sensing (*20*). The direction and magnitude of the change make it distinguishable from effects due to changes in electrode geometry resulting from stretch.

In addition, we make the sensor transparent, opening the possibility of touch screen functionality. Some sensors have been made transparent (*8*–*10*, *21*, *22*), and stretchable light-emitting surfaces (*23*) and displays (*24*) have also been created. In creating a surface that is sensitive to a finger and that is transparent but is also relatively insensitive to deformation, we hope to pave the way for stretchable touch screens that could be worn or applied to any surface. To make the device flexible, stretchable, and transparent, we use ion-containing hydrogels as electrodes, as recently demonstrated by Keplinger *et al.* (*25*). This ionic skin (*6*) approach does not suffer from the trade-off between conductance and optical transmission found with metals and semiconductors because the material acts as a dielectric at optical wavelengths, with high transparency even for a centimeter thickness [98%, not including surface reflections (*25*)]. Although the conductivity of these gels is 1000 times lower than that of indium tin oxide, in applications where film thickness of a few hundreds of micrometers is acceptable or only small currents are needed (as in capacitive sensing), the lower conductivity is not constraining. Sun *et al.* (*6*) showed that these electrodes can sense stretch or touch because of a change in the dimensions when the gel electrodes form a parallel plate capacitor. The area of the plates and the separation between them are modified upon deformation, leading to a change in the capacitance that is measured. A disadvantage of this approach is that it is not possible to determine whether the change is due to a stretch or a touch, and as a result, the device operates only to detect one or the other. Recent work in which four electrodes are attached to a transparent sheet of a highly deformable conductive gel, one to each corner, reports the detection of touch and of stretch (*26*). In this elegantly simple approach, the relative resistances between the electrodes and the finger—acting as a current return path—are used to estimate the position of the finger. This method, which has previously been implemented in conducting fabrics (*27*, *28*), does suffer

Department of Electrical and Computer Engineering, University of British Columbia, Vancouver, British Columbia V6T1Z4, Canada.
*Corresponding author. Email: jmadden@ece.ubc.ca

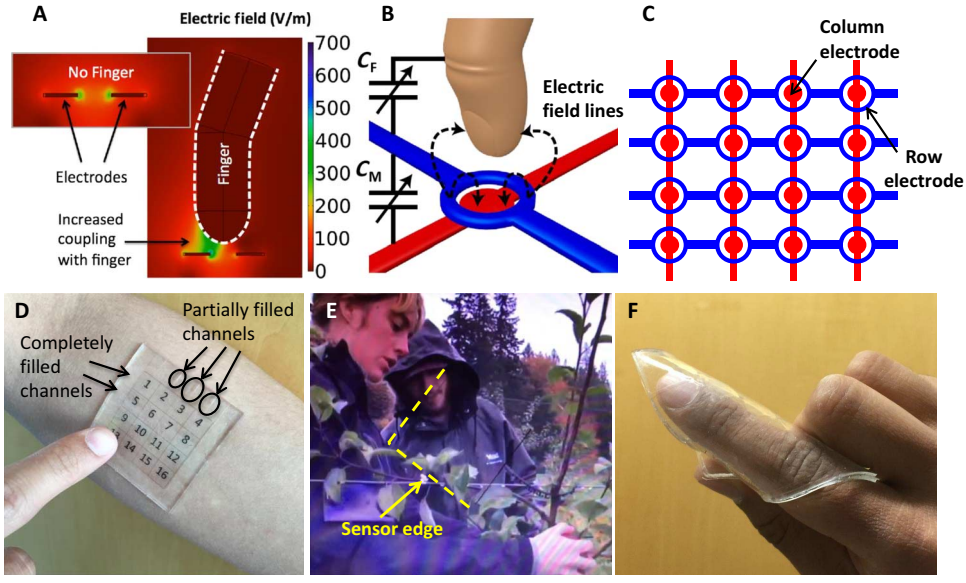

Fig. 1. Working principle and general properties. (**A**) Mutual capacitive coupling is simulated between two planar electrodes (shown in the inset without a finger). The coupling between electrodes is reduced by the presence of a finger, which acts as an electrode itself. (**B**) Finger approaching a pair of electrodes that are in the form of a loop and disc. The finger reduces the coupling between the electrodes (C_M) by coupling itself with the projected field (C_F is increased). (**C**) Two-dimensional array of loop-disc electrode pattern, with the loops on top. (**D**) Sensor array sitting above a forearm and a printed number pad. (**E**) Sensor array on an LCD with a video playing demonstrating transparency. Two edges of the sensor are indicated by the dashed lines. A third edge is just visible, extending perpendicular to the lower line. (**F**) Sensor array wrapped around a finger demonstrating conformity.

from distortions in the position mapping, particularly when stretch is nonuniform (as the inverse problem is ill-posed), which is ill-suited for a wearable trackpad or touch screen. Also, it does not offer an ability to distinguish simultaneous multiple finger touch. Here, we instead demonstrate the use of projected electric fields, which strongly interact with approaching fingers, making it easy to distinguish finger touch from stretching and bending. The sensors are patterned into an array, enabling lateral position localization. This approach also allows for the possibility of integrating other sensors, including pressure, bend, and stretch sensors, to enable a complete mapping of the sensor surface and its surroundings.

RESULTS

A cross-grid array of ionically conductive hydrogel electrodes is created with the electrodes capacitively coupled through a silicone elastomer matrix, producing a field that extends beyond the surface of the device. In this implementation, each array element is composed of a disc-shaped electrode and its interconnections (Fig. 1B, red) separated from a loop electrode (Fig. 1B, blue) by a dielectric layer. The loop and disc coupling allows for better vertical projection of the field than a simple crossing of lines. The finger acts as a third electrode, which capacitively couples to the sensor element, as represented by the variable capacitor C_F in Fig. 1B, reducing the coupling between electrodes, C_M. These loop and disk elements are placed in a sensor array (depicted in Fig. 1C) made of transparent and deformable materials, as evident in Fig. 1 (D to F). An array is shown in Fig. 1D on a forearm with a printed number pad under it to illustrate the transparency. Three channels are left with unfilled regions to demonstrate how filling makes these channels nearly invisible. The sensor is placed on a liquid crystal display (LCD) playing a video in Fig. 1E to demonstrate that the sensor is barely detectable. The edges are highlighted by dashed lines and labeled as "sensor edges." Figure 1F shows the sensor wrapped around a finger, an indication of its conformability.

The materials and methods are deliberately chosen to be low cost and appropriate for large-format mass production. A simple three-step fabrication process, mold-bond-polymerize (MBP; Fig. 2, A to C), produces a unibody sensor. The fabrication process is similar to that used in microfluidics device fabrication (*29*–*31*) to mass produce products such as lab-on-chip devices (*32*). Polyacrylamide, the hydrogel used to form the electrodes, is widely used in cosmetics and DNA gel electrophoresis. An ionic resistivity of 0.06 ohm·m (measured for a 2.74 M concentration of NaCl) is established by the presence of the salt in the hydrophilic polymer that contains 90% water. The dielectric that surrounds the electrodes is the widely available silicone elastomer polydimethylsiloxane (PDMS).

In the MBP process flow developed to fabricate the sensor, PDMS is first cured in a mold (Fig. 2A), and then released, forming a 700-μm-thick layer with 400-μm-deep grooves. These grooves are to contain the ionically conductive yet transparent and flexible interconnect "wires" of the capacitive sensor array. The layer is plasma-bonded (*33*, *34*) to an unpatterned 400-μm-thick uniform PDMS dielectric sheet to form an assembly with miniature channels. The process is repeated to form perpendicular channels (Fig. 2B). The final PDMS shell with perpendicularly running channels has crossover points (referred to as tactile pixels or taxels) 5 mm apart from each other. The number of contacts in the cross-wire array approach is $2n$ for the case of an array of $n \times n = n^2$ taxels. In the proposed architecture, the space consumed by the interconnects is minimal when the array size is scaled up, especially compared to structures that have two distinct electrodes for each sensor element. In the case demonstrated here, the number of taxels is 16, and the number of lines is 8, with 4 on each axis. Each taxel element has a diameter of 5 mm. A monomer mixture with a salt (NaCl in this case) is injected in the channels and polymerized to form

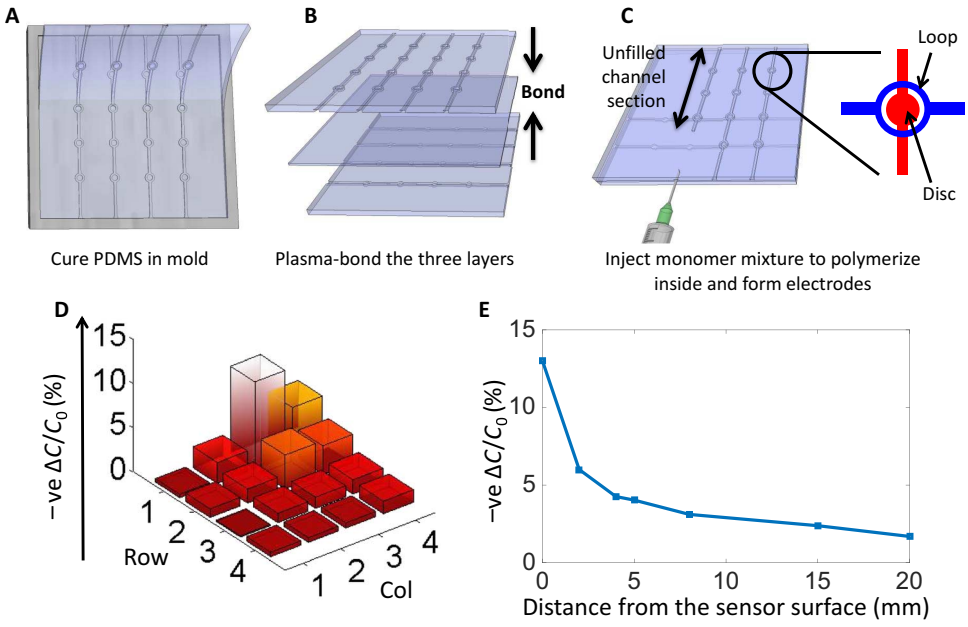

Fig. 2. Sensor fabrication and sensitivity. (**A**) Curing PDMS in a mold. (**B**) Plasma-bonding three layers forming perpendicular channels on top and bottom of the dielectric. (**C**) Injecting the monomer mixture inside the channels and polymerizing them to form the ionically conducting electrodes. (**D**) Map showing the localized change in capacitance due to a touch by a finger. (**E**) Change in capacitance due to a hovering finger at various distances from the top of the sensor. The change in capacitance upon approach of the finger is negative, as indicated.

the ionically conductive electrodes (Fig. 2C). Water will evaporate through the PDMS over the course of a day, which can be prevented by using LiCl electrolyte in the gel (*35*). A glycerol NaCl solution has also been used in place of the gel to avoid evaporation.

The transmittance of the freestanding sensor in air is measured to be 90%. The light attenuation includes reflective losses at the air-sensor interfaces due to refractive index mismatch (estimated to account for 6% of the 10% loss) and at the hydrogel-PDMS interfaces (less than 1% loss). The remaining 4% loss is primarily the result of surface imperfections. Both surface scattering and reflections should readily be reduced by adding antireflection coatings (*36*) and using molds with an optical finish. When the sensor is placed on a surface of relatively high index, such as on an LCD, as shown in Fig. 1E, the reflection losses and surface scattering effects are essentially halved, which helps explain why it is difficult to see the sensor (that is, the sensor is transparent).

To detect single or multi-touch with a small number of electrical connections, the mutual capacitance concept is implemented (as shown in Fig. 1B and C). The lateral position of a finger can be detected on the basis of the capacitance changes observed. Each combination of row and column electrodes is scanned sequentially, and the capacitances of all taxels are determined to create a map (as shown in Fig. 2D), in this case indicating the presence of the finger at the intersection of row 1 and column 3, that is, element (1,3). The loop and disk design of the electrodes depicted in Fig. 1B is such that the fringe field exposed to an approaching finger is large, thereby bringing about a significant change in capacitance due to the presence of the finger. When the finger reaches the interface, it yields a 13% decrease in capacitance at the taxel being activated (Fig. 2D, white shaded bar). Unlike other conformable capacitive sensor implementations, in this approach, no force is required to obtain the change in signal. The proximity approach allows for noncontact gestures to be detected, as in Samsung's "Air View." Contact gestures such as the translational motion of a finger on the sensor surface, commonly referred to as a "swipe," can also be sensed without the need to press firmly, minimizing stiction on the soft surface. In the previous designs, including the recent use of gel electrodes (*6*), touch sensitivity is achieved by physical deformation, which also leads to sensitivity to stretch, and may explain why these works have not presented the ability to detect touch during stretch. The fringing fields result in some sensitivity also in the neighboring taxels (as seen from the map in Fig. 2D). Each bar in the map corresponds to a loop-disc taxel arranged as in Fig. 2C.

To investigate the proximity detection capabilities of the sensor, we clamped a finger in a fixed position, and the sensor array, placed on an elevator stage, was vertically moved closer to the finger. The clamping not only determines relative sensor-finger vertical position but also holds the lateral position fixed. The corresponding capacitances were recorded. Figure 2E shows the relative magnitude of the change in capacitance as a function of distance from the surface. The sensor is demonstrated to be highly sensitive to a finger in very close proximity (lightly touching the surface). The change in capacitance falls off when the finger is further from the surface but is still significant even at 2 cm. Movie S1 shows the detection of proximity.

To determine the sensitivity of touch sensing to stretching, we clamped the sensor in a dynamic mechanical analyzer. A controlled sinusoidal stretch of 5-mm amplitude (corresponding to a strain of 7%) at 0.11 Hz was applied, and the corresponding capacitance was recorded. The stretch and the result of touch during stretch are shown in Fig. 3A, with the sinusoidal stretch onset after 40 s. It is observed that the capacitance increases with a stretch and follows the magnitude of the strain. Some change in capacitance is expected from the increase in overlapping electrode area and the reduction in dielectric thickness brought about by the stretch. While being stretched, the sensor was lightly touched three times between 65 and 110 s after the start of measurement (as shown in Fig. 3A). This brought about a significant

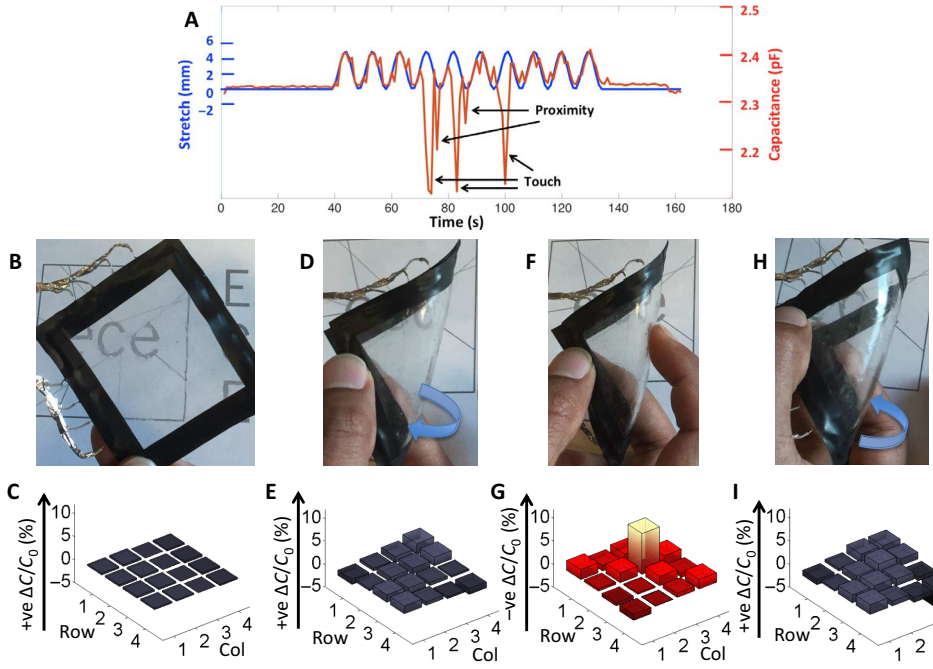

Fig. 3. Touching while stretching and bending. (**A**) Plot showing the recorded displacement (7% strain) and capacitance of a single taxel in the sensor while being stretched by a sinusoidally varying displacement using a dynamic mechanical analyzer; the sharp drops in capacitance coincide with touch, while the sinusoidally varying changes are the result of the stretching. (**B**) Sensor in steady state. (**C**) Stable capacitance map for steady state. (**D**) Sensor folded in an anticlockwise direction. (**E**) Resulting small positive change in capacitance of the taxels along the axis of bend where capacitance increases with positive *y* axis. (**F**) Sensor being touched while being bent. (**G**) Negative change in capacitance map showing the taxel touched having a change in capacitance of 10%, reduced slightly by the change due to the bend where the capacitance decreases with positive *y* axis. (**H**) Sensor being bent in the clockwise direction. (**I**) Positive change in capacitance map showing the axis of bend and a similar response that in (E).

decrease in capacitance. The finger contact signal is much larger than the change due to stretching. There is some jitter in the touch response because the finger itself bounces upon contact. Movie S2 shows the stretch and simultaneous finger detection process.

To investigate the effects of bending, we folded the sensor array from the planar state shown in Fig. 3B, in which capacitance is uniform, to a state in which the right hand corner is brought up toward the camera viewpoint, leading to a small radius of curvature (~10 mm) along the bend line (seen in Fig. 3D). Figure 3E shows a small increase (~2%) in capacitance along the fold line. The relative immunity to bending is not surprising because the thickness of the dielectric (400 μm) is much smaller than the bending radius of curvature (10 mm), leading to approximately ±2% strain in the top and bottom electrodes. The sensor is touched while being bent, as shown in Fig. 3F, and the resulting change in capacitance is plotted in Fig. 3G, which shows a large decrease in capacitance at the location of the touch, indicating easy detection of the touch during bending. In the figure, the vertical axis shows a negative change in capacitance, whereas in the neighboring plots, the change in capacitance is positive, with the vertical axis being positive change and this change is represented by dark blue instead of red and yellow. Finally, folding of the sensor array in the opposite direction (Fig. 3H) yields a similarly small increase in capacitance along the axis of bend (Fig. 3I) as that seen with the opposing fold. These demonstrations of detection of a finger while being actively stretched and/or bent are important in applications where the device may be folded as part of its normal use, such as application to the surface of a flexible display to create a touch screen. Movie S3 shows the sensor array operating in bending.

The sensor is able to detect gestures such as a swipe, where a finger in light contact with the sensor is moved across the array (as shown in Fig. 4A). The use of projected fields makes the approach very sensitive to such gestures, where there is only very light contact. The $\Delta C/C_0$ maps in Fig. 4A show that the finger partially activates neighboring taxels, which can be used to find the center of mass of the activation using further signal processing to enhance the spatial resolution, if needed. Another common gesture used in commercial touch screen devices is the multitouch capability (shown in Fig. 4B), in which the presence of one, two, and then three fingers is detectable. Movies S4 and S5 demonstrate detection of finger translation and of multitouch.

The design of the electrodes makes the sensor relatively immune to bending and stretch, whereas the presence of a finger is strongly captured. This is made possible by the electrode pattern (loop and disc in this case, which projects field) and the use of a relatively thin sheet with the positive and negative electrodes equally spaced on either side of the neutral axis (which reduces sensitivity to bending). In some cases, it is desirable to determine the overall shape of the surface. The sensitivity to bending can be increased if desired by modifying the geometry. Figure 4C shows the increased response to bending achieved when the electrodes are offset relative to the neutral axis, so their strains are no longer equal and opposite during bending. In this case, the top layer is made thicker such that the neutral axis is aligned with the top electrode layer instead of the dielectric, so the bottom electrode layer would experience a large strain and thereby detect a bend more readily. The radius of the curvature in Fig. 4C is ~10 mm. As seen from the cross-sectional diagram in Fig. 4C, the bottom electrode layer is 640 μm away from the neutral axis and therefore experiences a

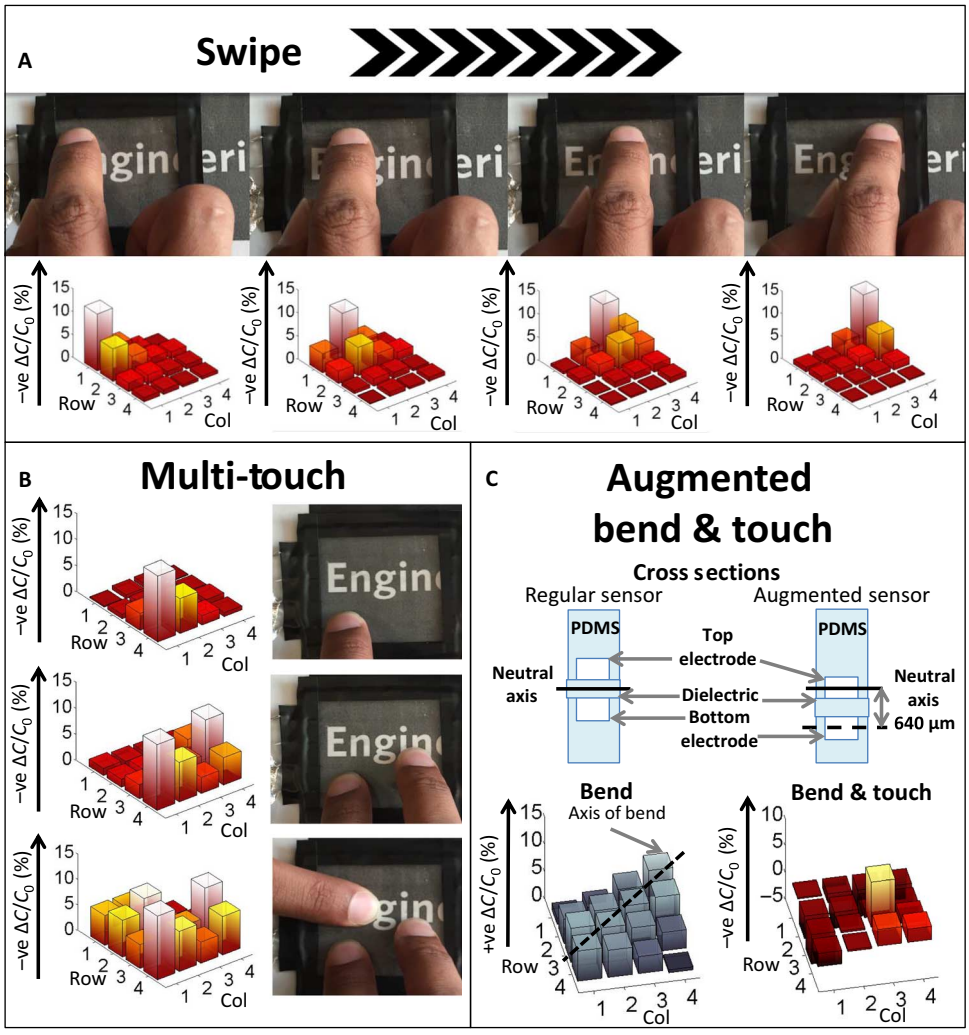

Fig. 4. Swipe, multitouch, and augmented bend detection. (**A**) Swipe functionality of the sensor showing the negative change in capacitance following a movement across the row from left to right. (**B**) Detection of one (top), two (middle), and three (bottom) fingers simultaneously, demonstrating multitouch capability. (**C**) Diagram of the design and results from an augmented bend sensor (compared with the regular sensor with the neutral axis aligned with the dielectric), with the neutral axis aligned with the top electrode layer, which enhances the detection of bend (bottom left) but still enables the simultaneous detection of touch (bottom right).

strain of ~6.4% (whereas the top electrode remains unstrained being on the neutral axis). This results in a larger change in capacitance (~5%) compared to the previous iteration (~2%) with the dielectric along the neutral axis (Fig. 3, D to I). The grayscale plot in Fig. 4C shows the axis of bend corresponding to the bending action in the image above it. Under bent conditions, the sensor is still able to detect a touch, as seen from the rightmost image in Fig. 4C. This opens the possibility of designing the sense electrodes to be more or less sensitive to particular modes of deformation or touch. There is the possibility of making certain elements more sensitive to bending or stretching while making other elements less sensitive by modifying, for example, their geometry and neutral axis offset, which would enable complete reconstruction of the surface conformation.

A potential challenge with any multilayer composite structure such as the sensor arrays is failure by delamination. An initial study of the general robustness of the sensor array was performed, in which the sensor was clamped and stretched by 10%, followed by a buckle with a radius of curvature of 16 mm (corresponding to a surface strain of 6%). After half a million cycles, the sensor still continued to function without any noticeable degradation to the change in capacitance, as observed in response to a light finger touch, and with no apparent delamination. The results are described in the Supplementary Materials, and the sensitivity to touch as a function of cycle number is plotted in fig. S5. The sensor array was also heated to 80°C for 15 min and cooled to −10°C for 15 min. Following these temperature exposures, the sensor responded to a touch as before (the taxel sensitivity was initially 14%, and afterward was 13%, within the typical variation range resulting from slight changes in finger position and orientation). The array is also resistant to common environmental contamination such as a coffee spill, as shown in the video in movie S6.

DISCUSSION

The sensor is seamless in appearance and visually transparent with swipe and multitouch detection capabilities. Finger contact leads to a decrease in capacitance, whereas a stretch causes the capacitance

to increase with a magnitude much smaller in comparison to the change brought about by a touch, enabling ready differentiation of the two stimuli. The capacitance also changes by a relatively small amount in response to a bend, with the sensitivity to bending augmented by changing the alignment of the neutral axis. In its current form, the sensor is not highly sensitive to pressure because of its geometry and the relative stiffness of the dielectric (~1 MPa). The sensor structure can be altered to increase pressure sensitivity by, for example, having a parallel plate geometry for each capacitor, as is typical in other designs (*6*, *8*, *9*). However, pressure-sensitive geometries will also be susceptible to stretch. A mixture of both pressure and projected capacitance sensors could provide combined information enabling finger location and applied pressure detection, including the discrimination of stretch-, bend-, and touch-related deformations.

To be effective for portable and mobile applications, sensing devices should be of low power, and the footprint of the interface electronics should be small to facilitate compact-form factors. Here, the readout electronics is based on well-established capacitive sensor readout circuits that are widely used in mobile devices. Although we used an Arduino platform together with a capacitance-to-digital converter (CDC) chip, a custom single-chip solution can be envisioned that has approximately double the 5-mm × 6-mm footprint of the CDC and has an average power consumption of less than 1 mW. At this power level and with 8 hours of continuous operation per day, the proposed system can be expected to last 3 months without recharging using a typical smartwatch battery.

Cost of materials and fabrication are particularly important for wearables, especially those that are disposable or add value to already low-cost products. A promising aspect of the current technology is its combination of low-cost materials (~$1/m^2) and the low-cost, scalable fabrication process, proven in microfluidics (*29*–*31*). Low cost also makes the use of this technology for large-area coverings interesting. Keplinger *et al.* (*25*) have shown that gel-based ionic conductor pairs can propagate signals with a highly effective diffusion rate. For the sensor array case, a limit on the maximum dimensions of the sensor is set by the *RC* time constant of the most distant taxel, the refresh time, τ, and the number of taxels, *n*. The *RC* time constant is important because if a taxel is probed on too short a time scale or at too high a frequency, the resistance of the interconnects will dominate and the capacitive signal will be small. Assuming the taxels are individually addressed sequentially, the *RC* time constant should be less than or approximately equal to the measurement time for each taxel, given by τ/*n*. The maximum sensor array dimension, L_{max}, is then approximately

$$L_{max} \leq \sqrt[3]{\frac{\sigma \alpha l t_i t_d \tau}{2\beta \varepsilon_r \in_0}} \quad (1)$$

In this equation, a square array is assumed with the dimension of each taxel being $l \times l$, the conductivity of the interconnects is represented by σ, the thickness of the interconnect is t_i and that of the dielectric is t_d, and the permittivity of the dielectric is $\varepsilon_r\varepsilon_o$. Here, αl is the average width of each interconnect (with α being the fraction of the width consumed by the interconnect), whereas β represents the ratio of the taxel and parasitic capacitance to that of an $l \times l$ parallel plate capacitor. As expected, increasing the width of the conductor, αl, and the thickness, t_i, will allow the size to be increased by reducing resistance of the conductor. Increasing the capacitance by reducing the dielectric thickness or increasing the permittivity will reduce the dimensions. The estimate in Eq. 1 suggests that the sensor array area can be very large, approximately 50 m × 50 m in a 20-cm grid refreshed every half a second. Such a format might be used to detect the presence of feet (instead of fingers).

An attractive feature of any capacitive technology is that its resolution scales in proportion to the dimension of the electrodes. Like a parallel plate capacitor whose dimensions are uniformly scaled up or down, the magnitude of the projected capacitance also scales linearly, as do the vertical and lateral resolutions (discussed in the Supplementary Materials). Devices can be constructed to sense at much larger or smaller scales than the millimeter levels shown here, subject of course to limitations of fabrication methods and instrumentation considerations. Microelectromechanical system devices sense capacitances that are 1000 times smaller (*37*) than those of our devices, suggesting that operation with micrometer resolution is possible if desired.

With flexible displays having been implemented by Sony, Samsung, Plastic Logic, and others, and with stretchable electroluminescent materials and displays emerging (*23*, *24*), it is interesting to consider how these interfaces can be made interactive. The transparent sensor array, when laminated onto the surface of a deformable display, promises to enable touch screen selection and gesture-based interactions even during bending and stretching. If the device is also made sensitive to stretch (independently), image distortion could be corrected. A rudimentary example of a transparent application is shown in movie S7, in which finger touch is used to signal the activation of underlying light-emitting diodes (LEDs) on a wristband. In general, the compliance and transparency offer the promise of applying the sensor arrays to virtually any surface.

MATERIALS AND METHODS

Fabrication of sensor

PDMS (Sylgard 184 silicone elastomer) was mixed in a 10 (base):1 (cross-linker) ratio and then degassed to get rid of the air bubbles. The uncured mix was then poured into molds, and the molds were then placed into an oven at 80°C for an hour. The molds were made of aluminum and formed films that were 55 mm × 55 mm across and 700 μm in thickness. The cured PDMS films with patterned grooves were then peeled off. The molds contained 1-mm-wide and 400-μm-deep channels that formed the gel interconnects between the loops (top electrodes) or discs (bottom electrodes). The discs were 1.2 mm in diameter, whereas the loops had an outer diameter of 5 mm and an inner diameter of 3 mm. The loops and discs were 400 μm deep. A uniform-thickness middle dielectric layer was obtained by spin coating a 400-μm-thick uncured PDMS layer on a silicon wafer at 300 rpm for 20 s. The dielectric was then similarly cured at 80°C for an hour. The three cured layers were then plasma-bonded using a Harrick Plasma Cleaner (PDC-001) by exposing the surfaces to be bonded to oxygen plasma at a pressure of 600 mtorr for 110 s. We also demonstrated the bonding of layers using partially cured PDMS and ultraviolet (UV)–curable adhesive (*32*). A solution containing 2.2 M acrylamide (AAm) (A8887, Sigma-Aldrich) and 2.74 M NaCl was prepared. The concentrations of AAm and NaCl were similar to those used by Sun *et al.* (*6*). Ammonium persulfate [AP; 1.5 weight % (wt %)] (A9164, Sigma-Aldrich) was added as an initiator, and 0.06 wt % of the cross-linker *N*,*N*-methylenebisacrylamide (M7279, Sigma-Aldrich) was dissolved, with respect to the weight of the AAm monomer. The mixture was then degassed. *N*,*N*,*N*′,*N*′-tetramethylethylenediamine (TEMED; 1.0 wt %)

(T7024, Sigma-Aldrich) was added as the accelerator, causing rapid polymerization. The stoichiometry of AP and TEMED was developed for specifically timed polymerization. Upon the addition of the accelerator, the mixture was injected into the channels within 1 min, and the mixture polymerized as it flowed through the channels. The process was timed such that the polymerization was completed as the channel was filled. Finally, silver-plated copper wires with a diameter of 250 μm were inserted into the openings of the channels, and the channels were then sealed using silicone epoxy (Sil-Poxy from Smooth-On).

Sensor readout

An Analog Devices CDC chip (AD7746) was used to read the capacitance. The CDC was essentially a Delta-Sigma analog-to-digital converter (ADC). In this case, a constant voltage input was used, whereas the feedback capacitor of the integrator was the sense capacitor. The change in the feedback capacitance resulted in a change in the digital output at constant input voltage. Two multiplexers (MAX 4518) were used to cycle through the eight electrodes, and the output of the multiplexers was fed to a microcontroller (Arduino Mega 2560). The microcontroller controlled the multiplexers and CDC and fed the final data through a serial port into a computer where digital values of the capacitance could be acquired and displayed. The entire 4 × 4 array of 16 taxels was sampled three times per second. A form of running averaging of the signal was carried out to attenuate effects of noise and drift in the signal.

Resistivity measurement

A rectangular block of polyacrylamide was fabricated with a 2.74 M concentration of NaCl. Two electrodes attached to the ends of the gel block were connected to an LCR meter (HP 4275A) to measure the impedance at different frequencies (10, 20, and 40 kHz), which was then used to calculate the resistivity of the gel block of known dimensions.

Transmission measurement

The sensor was placed inside the holding zone in a Hitachi U-3010 UV-visible spectrophotometer, and the transmission was measured with air as the baseline. Transmission was through a region including both hydrogel and PDMS.

Mechanical cycle characterization

The sensor was clamped with the effective length of the sensor between the clamps set at 20 mm. The entire setup was submerged in water to ensure the consistency of hydration. The mechanical analyzer was then used to apply a 2-mm amplitude sine wave (10% strain) followed by a buckling of the sensor by a radius of curvature of approximately 16 mm (corresponding to a surface strain of 6%) at 1 Hz for 500,000 cycles, as described more fully in the Supplementary Materials.

Thermal characterization

The sensor was placed in a water bath and heated up to 80°C and held for 15 min. Upon returning to room temperature, it was tested and was fully functional. The sensor was then placed in a beaker with car antifreeze (working ingredient was ethylene glycol) in it, and a Thermo Scientific Neslab CC65 immersion cooler was used to cool it to −10°C and held for 15 min. Upon returning to room temperature, its functionality was judged on the basis of the sensitivity to light finger touch (in percent increase in capacitance).

SUPPLEMENTARY MATERIALS

Supplementary material for this article is available at http://advances.sciencemag.org/cgi/content/full/3/3/e1602200/DC1

Effects of scaling on sensor

Mechanical characterization: Cyclic loading

fig. S1. Coplanar electrode capacitor with a finger.

fig. S2. Finger on an array of capacitive sensors.

fig. S3. Effect of scaling on change in capacitance along a row due to a touch at a single taxel.

fig. S4. Steps of mechanical test.

fig. S5. Plot showing change in capacitance in percentage due to a touch after cycles of 10% strain, followed by a buckling with a radius of curvature of 16 mm.

movie S1. Video showing proximity detection.

movie S2. Video showing the sensor being stretched and then being touched while being stretched.

movie S3. Video showing the sensor being bent and a finger touching it while bending.

movie S4. Video showing a finger moving across the sensor and the sensor's response to it.

movie S5. Video showing multiple fingers touching the sensor at multiple locations.

movie S6. Video showing an accidental coffee spill on the sensor and continued functionality after wiping it clean.

movie S7. Video showing a wrist gear made using this sensor and an LED grid under it to demonstrate potential use as part of a wearable device.

Reference (*38*)

REFERENCES AND NOTES

1. D. De Rossi, Electronic textiles: A logical step. *Nat. Mater.* **6**, 328–329 (2007).
2. S. Xu, Y. Zhang, L. Jia, K. E. Mathewson, K.-I. Jang, J. Kim, H. Fu, X. Huang, P. Chava, R. Wang, S. Bhole, L. Wang, Y. J. Na, Y. Guan, M. Flavin, Z. Han, Y. Huang, J. A. Rogers, Soft microfluidic assemblies of sensors, circuits, and radios for the skin. *Science* **344**, 70–74 (2014).
3. T. Someya, Building bionic skin. *IEEE Spectr.* **50**, 50–56 (2013).
4. D. Xu, A. Tairych, I. A. Anderson, Where the rubber meets the hand: Unlocking the sensing potential of dielectric elastomers. *J. Polym. Sci. Part B Polym. Phys.* **54**, 465–472 (2016).
5. X. Wang, L. Dong, H. Zhang, R. Yu, C. Pan, Z. L. Wang, Recent progress in electronic skin. *Adv. Sci.* **2**, 1500169 (2015).
6. J.-Y. Sun, C. Keplinger, G. M. Whitesides, Z. Suo, Ionic skin. *Adv. Mater.* **26**, 7608–7614 (2014).
7. T. Someya, T. Sekitani, S. Iba, Y. Kato, H. Kawaguchi, T. Sakurai, A large-area, flexible pressure sensor matrix with organic field-effect transistors for artificial skin applications. *Proc. Natl. Acad. Sci. U.S.A.* **101**, 9966–9970 (2004).
8. W. Hu, X. Niu, R. Zhao, Q. Pei, Elastomeric transparent capacitive sensors based on an interpenetrating composite of silver nanowires and polyurethane. *Appl. Phys. Lett.* **102**, 83303 (2013).
9. E.-S. Choi, M.-H. Jeong, K. W. Choi, C. Lim, S.-B. Lee, Flexible and transparent touch sensor using single-wall carbon nanotube thin-films, in *Third International Nanoelectronics Conference*, Hong Kong, 3 to 8 January 2010.
10. M. S. us Sarwar, Y. Dobashi ; E. F. S. Glitz, M. Farajollahi, S. Mirabbasi, S. Naficy, G. M. Spinks, J. D. W. Madden, Transparent and conformal 'piezoionic' touch sensor, in *Proceedings of SPIE: Electroactive Polymer Actuators and Devices (EAPAD)*, Y. Bar-Cohen, Ed. (International Society for Optics and Photonics, 2015); http://proceedings.spiedigitallibrary.org/proceeding.aspx?articleid=2239762.
11. D. J. Cohen, D. Mitra, K. Peterson, M. M. Maharbiz, A highly elastic, capacitive strain gauge based on percolating nanotube networks. *Nano Lett.* **12**, 1821–1825 (2012).
12. L. Cai, L. Song, P. Luan, Q. Zhang, N. Zhang, Q. Gao, D. Zhao, X. Zhang, M. Tu, F. Yang, W. Zhou, Q. Fan, J. Luo, W. Zhou, P. M. Ajayan, S. Xie, Super-stretchable, transparent carbon nanotube-based capacitive strain sensors for human motion detection. *Sci. Rep.* **3**, 3048 (2013).
13. C. Pang, G.-Y. Lee, T.-i. Kim, S. M. Kim, H. N. Kim, S.-H. Ahn, K.-Y. Suh, A flexible and highly sensitive strain-gauge sensor using reversible interlocking of nanofibres. *Nat. Mater.* **11**, 795–801 (2012).
14. D. J. Lipomi, M. Vosgueritchian, B. C.-K. Tee, S. L. Hellstrom, J. A. Lee, C. H. Fox, Z. Bao, Skin-like pressure and strain sensors based on transparent elastic films of carbon nanotubes. *Nat. Nanotechnol.* **6**, 788–792 (2011).
15. S. Park, H. Kim, M. Vosgueritchian, S. Cheon, H. Kim, J. H. Koo, T. R. Kim, S. Lee, G. Schwartz, H. Chang, Z. Bao, Stretchable energy-harvesting tactile electronic skin capable of differentiating multiple mechanical stimuli modes. *Adv. Mater.* **26**, 7324–7332 (2014).
16. H.-H. Chou, A. Nguyen, A. Chortos, J. W. F. To, C. Lu, J. Mei, T. Kurosawa, W.-G. Bae, J. B.-H. Tok, Z. Bao, A chameleon-inspired stretchable electronic skin with interactive colour changing controlled by tactile sensing. *Nat. Commun.* **6**, 8011 (2015).

17. X. Wang, T. Li, J. Adams, J. Yang, Transparent, stretchable, carbon-nanotube-inlaid conductors enabled by standard replication technology for capacitive pressure, strain and touch sensors. *J. Mater. Chem. A* **1**, 3580–3586 (2013).
18. J. Kim, M. Lee, H. J. Shim, R. Ghaffari, H. R. Cho, D. Son, Y. H. Jung, M. Soh, C. Choi, S. Jung, K. Chu, D. Jeon, S.-T. Lee, J. H. Kim, S. H. Choi, T. Hyeon, D.-H. Kim, Stretchable silicon nanoribbon electronics for skin prosthesis. *Nat. Commun.* **5**, 5747 (2014).
19. B. Li, A. K. Fontecchio, Y. Visell, Mutual capacitance of liquid conductors in deformable tactile sensing arrays. *Appl. Phys. Lett.* **108**, 13502 (2016).
20. G. Walker, A review of technologies for sensing contact location on the surface of a display. *J. Soc. Inf. Disp.* **20**, 413–440 (2012).
21. B. Zhang, Z. Xiang, S. Zhu, Q. Hu, Y. Cao, J. Zhong, Q. Zhong, B. Wang, Y. Fang, B. Hu, J. Zhou, Z. Wang, Dual functional transparent film for proximity and pressure sensing. *Nano Res.* **7**, 1488–1496 (2014).
22. C. Gu, S. Chen, X. Guo, Transparent elastic capacitive pressure sensors based on silver nanowire electrodes. *8th Annu. IEEE Int. Conf. Nano/Micro Eng. Mol. Syst.* **1**, 1183–1185 (2013).
23. C. Larson, B. Peele, S. Li, S. Robinson, M. Totaro, L. Beccai, B. Mazzolai, R. Shepherd, Highly stretchable electroluminescent skin for optical signaling and tactile sensing. *Science* **351**, 1071–1074 (2016).
24. T. Sekitani, H. Nakajima, H. Maeda, T. Fukushima, T. Aida, K. Hata, T. Someya, Stretchable active-matrix organic light-emitting diode display using printable elastic conductors. *Nat. Mater.* **8**, 494–499 (2009).
25. C. Keplinger, J.-Y. Sun, C. C. Foo, P. Rothemund, G. M. Whitesides, Z. Suo, Stretchable, transparent, ionic conductors. *Science* **341**, 984–987 (2013).
26. C.-C. Kim, H.-H. Lee, K. H. Oh, J.-Y. Sun, Highly stretchable, transparent ionic touch panel. *Science* **353**, 682–687 (2016).
27. A. Schmeder, A. Freed, Support vector machine learning for gesture signal estimation with a piezo-resistive fabric touch surface, in *Proceedings of International New Interfaces for Musical Expressions (NIME'10)*, Sydney, Australia, 15 to 18 June 2010.
28. A. Flagg, K. E. MacLean, Affective touch gesture recognition for a furry zoomorphic machine, in *Proceedings of the 7th International Conference on Tangible, Embedded and Embodied Interaction (TEI'13)*, Barcelona, Spain, 10 to 13 February 2013.
29. J. Friend, L. Yeo, Fabrication of microfluidic devices using polydimethylsiloxane. *Biomicrofluidics* **4**, 026502 (2010).
30. M. Lake, C. Narciso, K. Cowdrick, T. Storey, S. Zhang, J. Zartman, D. Hoelzle, Microfluidic device design, fabrication, and testing protocols. *Protoc. Exch.* **2015**, 10.1038/protex.2015.069 (2015).
31. S. K. Sia, G. M. Whitesides, Microfluidic devices fabricated in poly(dimethylsiloxane) for biological studies. *Electrophoresis* **24**, 3563–3576 (2003).
32. Y. Temiz, R. D. Lovchik, G. V. Kaigala, E. Delamarche, Lab-on-a-chip devices: How to close and plug the lab? *Microelectron. Eng.* **132**, 156–175 (2015).
33. M. A. Eddings, M. A. Johnson, B. K. Gale, Determining the optimal PDMS–PDMS bonding technique for microfluidic devices. *J. Micromech. Microeng.* **18**, 067001 (2008).
34. W. W. Y. Chow, K. F. Lei, G. Shi, W. J. Li, Q. Huang, Microfluidic channel fabrication by PDMS-interface bonding. *Smart Mater. Struct.* **15**, S112–S116 (2006).
35. Y. Bai, B. Chen, F. Xiang, J. Zhou, H. Wang, Z. Suo, Transparent hydrogel with enhanced water retention capacity by introducing highly hydratable salt. *Appl. Phys. Lett.* **105**, 151903 (2014).
36. Z. Wu, J. Walish, A. Nolte, L. Zhai, R. E. Cohen, M. F. Rubner, Deformable antireflection coatings from polymer and nanoparticle multilayers. *Adv. Mater.* **18**, 2699–2702 (2006).
37. J. Wei, C. Yue, Z. L. Chen, Z. W. Liu, P. M. Sarro, A silicon MEMS structure for characterization of femto-farad-level capacitive sensors with lock-in architecture. *J. Micromech. Microeng.* **20**, 064019 (2010).
38. R. Schinzinger, P. A. A. Laura, *Conformal Mapping: Methods and Applications* (Courier Corporation, 2003).

Acknowledgments: We thank M. Dawson for a thorough review of the manuscript and K. Ong and C. Ng for their aid in implementing the readout circuit and graphical user interface. **Funding:** This work was supported by a Natural Sciences and Engineering Research Council of Canada (NSERC) Collaborative Research and Development grant, an NSERC CGS grant (to M.S.S.), and an NSERC USRA and an NSERC Create (NanoMat) grant (to C.P.). **Author contributions:** M.S.S. and J.D.W.M. conceived the idea. M.S.S. simulated and designed the sensor, developed the fabrication process, and wrote the manuscript. M.S.S. and S.M. designed the readout circuit. Y.D. aided with fabrication and simulation. C.P. and J.K.M.W. aided in the fabrication and characterization of the sensor. All authors contributed in the review of manuscript. **Competing interests:** J.D.W.M., M.S.S., Y.D., C.P., J.K.M.W., and S.M. filed a patent application related to this work through the University of British Columbia on 3 December 2015 titled "Flexible transparent sensor with ionically-conductive material" (PCT/CA2015/051265). Authors will have financial benefits if the patent is sold or licensed. **Data and materials availability:** All data needed to evaluate the conclusions in the paper are present in the paper and/or the Supplementary Materials. Additional data related to this paper may be requested from the authors.

Submitted 11 September 2016
Accepted 2 February 2017
Published 15 March 2017
10.1126/sciadv.1602200

Citation: M. S. Sarwar, Y. Dobashi, C. Preston, J. K. M. Wyss, S. Mirabbasi, J. D. W. Madden, Bend, stretch, and touch: Locating a finger on an actively deformed transparent sensor array. *Sci. Adv.* **3**, e1602200 (2017).

Bend, stretch, and touch: Locating a finger on an actively deformed transparent sensor array

Mirza Saquib Sarwar, Yuta Dobashi, Claire Preston, Justin K. M. Wyss, Shahriar Mirabbasi and John David Wyndham Madden

Sci Adv **3** (3), e1602200.
DOI: 10.1126/sciadv.1602200